

Lyman-break galaxies: high mass or low?

Stephen J. Weatherley* and Stephen J. Warren

Astrophysics Group, Blackett Laboratory, Imperial College London, Prince Consort Road, London SW7 2BW, UK

Accepted 0000 January 00. Received 0000 January 00; in original form 0000 January 00

ABSTRACT

We reassess the hypothesis that Lyman-break galaxies (LBGs) at redshifts $z \sim 3$ mark the centres of the most massive dark matter haloes at that epoch. First we reanalyse the kinematic measurements of Pettini et al., and of Erb et al., of the rest-frame optical emission lines of LBGs. We compare the distribution of the ratio of the rotation velocity to the central line width, against the expected distribution for galaxies with random inclination angles, modelled as singular isothermal spheres. The model fits the data well. On this basis we argue that the central line width provides a predictor of the circular velocity at a radius of several kpc. Assembling a larger sample of LBGs with measured line widths, we compare these results against the theoretical Λ CDM rotation curves of Mo, Mao & White, under the hypothesis that LBGs mark the centres of the most massive dark matter halos. We find that the circular velocities are over-predicted by a substantial factor, which we estimate conservatively as 1.8 ± 0.4 . This indicates that the model is probably incorrect. The model of LBGs as relatively low-mass starburst systems, of Somerville, Primack, and Faber (2001), provides a good fit to the data.

Key words:

galaxies: kinematics and dynamics – galaxies: formation – galaxies: high redshift

1 INTRODUCTION

The rotation curves of galaxies have played, and continue to play, an important role in cosmology. The flat rotation curves of spiral galaxies at large radii (Babcock, 1939; Rubin, Thonnard & Ford, 1978; van Albada et al., 1985) were central to the construction of the modern paradigm that non-baryonic collisionless cold dark matter (CDM) dominates the matter density of the Universe. Within this paradigm, for specified cosmological parameters and a spectrum of initial density perturbations, and ignoring the baryons, the growth of structure in the dark matter can be modelled accurately (Lacey & Cole, 1993; Navarro, Frenk & White, 1997), providing predictions of the mass spectrum of dark matter halos at any redshift, and their density profiles. Recently, the rotation curves of low surface brightness galaxies have been used to test the predicted density profiles. Indeed, it has been argued that the inferred constant density cores are inconsistent with the cuspy density profiles predicted (de Blok, Bosma & McGaugh, 2003), perhaps indicating that a modification of the CDM paradigm is required. Alternatively the discrepancy may be an indication of the lack of understanding of how the density profile in the halo core is modified by the baryons, firstly in the collapse phase,

as well as in any subsequent phase of ejection of the baryons in a wind following star formation. Therefore there is a tie between progress in understanding the nature of the dark matter, and progress in understanding the assembly of the baryonic component of galaxies.

A similar tie exists in the study of galaxies at high redshift. The development of a successful method for identifying galaxies at $z \sim 3$, the Lyman-break technique (Steidel & Hamilton, 1993), and the measurement of the properties of the galaxies discovered (Steidel et al., 1996; 1998), allow further tests of the CDM paradigm. A simple hypothesis is that these Lyman-break galaxies (LBGs) mark the centres of the most massive dark matter halos. The benefit of this hypothesis is its simplicity, allowing detailed predictions. For example, by integrating the halo mass function down to the mass limit that produces a number density matching the number of LBGs, the distribution of halo masses is known, and the clustering strength can be predicted. Satisfactory agreement is found between the predicted clustering amplitude, and the measured value (Giavalisco et al., 1998; Adelberger et al., 1998, Mo, Mao & White, 1999).

An alternative view, promoted by Somerville, Primack, and Faber (2001, hereafter SPF) is that LBGs are starburst galaxies triggered by collisions. Since the starburst phase is short, under this hypothesis more halos contain a LBG at some time, and so the halo masses associated with LBGs

* Email : stephen.weatherley@imperial.ac.uk

are smaller. Kolatt et al. (1999), and Wechsler et al. (2001) show that this picture also provides a satisfactory explanation of the clustering properties of LBGs. Although many of the ingredients of this picture are uncertain, since galaxy collisions are in the nature of hierarchical galaxy formation, it would be surprising if there were not some truth in it.

To learn more about how the baryons in galaxies are assembled, and the nature of the dark matter, we need to discriminate between these two hypotheses. Clearly measurement of the masses of LBGs is the key to progress on these issues. Most of the useful kinematic information on LBGs comes from the measured line widths of rest-frame optical emission lines. However, because the stellar light in LBGs is very compact, with half-light radii of typically 0.2 arcsec (Marleau & Simard, 1998), these measurements sample the galaxy mass over the central few kpc only, where the mass is dominated by the baryons, and therefore where the circular velocity cannot be predicted reliably. For these reasons the measurement of a handful of rotation velocities at radii of nearly 1 arcsec, by Pettini et al. (2001), and Erb et al. (2003), are particularly useful, allowing direct comparison against the theoretical halo rotation curves, rather than the uncertain predicted stellar central velocity dispersions.

In this paper we reanalyse the kinematic data on LBGs, paying particular attention to those galaxies for which rotation velocities have been measured. We compare the results of this analysis against the predictions of Mo et al., (1999, hereafter MMW) of the halo rotation curves of LBGs under the hypothesis that LBGs mark the centres of the most massive dark matter halos. In Section 2 we assemble the kinematic data. In Section 3 we analyse the data on rotation velocities. We compare the distribution of the ratio of the rotation velocity to the central line width, against the expected distribution for galaxies with random inclination angles, modelled as singular isothermal spheres. The model fits the data well. On this basis we argue that the distribution of central line widths provides a reliable predictor of the distribution of circular velocities at radii of several kpc. We use this to infer the distribution of circular velocities for a larger sample of galaxies, for which only central line widths have been measured. In Section 4 we compare these circular velocities against the predictions of MMW, finding that the measured circular velocities are substantially smaller than the predicted values. Consideration of possible biases only reinforces this conclusion. We then compare our results against the collisional starburst model predictions of SPF, and find good agreement. Throughout, we assume a standard, flat Λ CDM cosmology with $\Omega_\Lambda = 0.7$ and $H_0 = 70 \text{ km s}^{-1} \text{ Mpc}^{-1}$. The same cosmology was used for the two models we compare against. For this cosmology an angle of 1 arcsec corresponds to the physical size 8.4 kpc at $z = 2$, and 7.7 kpc at $z = 3$.

2 LBG KINEMATIC DATA

In this section we assemble suitable kinematic data on LBGs for analysis. The rest-frame optical emission lines are the most useful for quantifying gravitational motions in LBGs. The Ly α emission line cannot be used because it is broadened by resonant scattering, while the strong interstellar absorption lines visible in rest-frame UV spectra are probably

broadened by non-gravitational motions and, in any case, are saturated. Any genuine stellar absorption lines are too weak to be useful.

Most of the kinematic information on LBGs is restricted to the measurement of the line widths. This is because, even in good seeing (~ 0.5 arcsec), from the ground the light profiles of most LBGs are spatially unresolved. There is still a relative paucity of these kinematic measures, largely due to the difficulty in detecting rest-frame optical emission which has been redshifted into the near-infrared. Therefore the strongest lines, [O III] and H α , are the most useful. The two largest samples of near-infrared spectra of LBGs are those of Pettini et al. (2001, hereafter P01), containing kinematic data on 16 galaxies, and of Erb et al. (2003, hereafter E03), also containing kinematic data on 16 galaxies. In Table 1 we summarise the relevant data on these 32 LBGs. Col. (1) provides the galaxy name, col. (2) the galaxy redshift, col. (3) the \mathcal{R} apparent magnitude, and col. (4) the emission-line velocity width, characterised by the standard deviation σ of a Gaussian fit, and its uncertainty (if provided in the original paper). In a few cases only upper limits are listed, as the lines were unresolved at the resolution of the observations. The emission line measured is listed in col. (5), and col. (6) provides the reference.

In a small number of cases the emission lines are spatially resolved, and show evidence of rotation. As argued above, these galaxies provide particularly valuable kinematic information. As emphasised by E03 the measurement of rotation in LBGs from the ground is difficult, because usually the galaxy half-light radius is smaller than the seeing. The two-dimensional structure of the emission line in the spectrum is therefore dominated by the kinematics near the centre of the galaxy. The effect of this is to smooth out the transition from +ve to -ve velocity in the rotation curve. For this reason we disregard the actual shape of the LBG rotation curves (e.g. Fig. 5, E03), and use only the quoted rotation velocity for each galaxy, taken as half the velocity difference between the two extreme points measured. Systematic biases in the measured rotation velocities are discussed in Section 4. Whether or not the rotation curve continues to rise after the last point does not concern us, since we will compare against predictions at the measured radii.

Details of the kinematic measures for the subset of eight galaxies with rotation velocities are provided in Table 2. In each case the authors provide both the central line width σ , and the rotation velocity V_r . In Table 2 the first four columns are the same as the first four columns of Table 1. Col. (5) lists the rotation velocity V_r , and col. (6) gives the ratio of the rotation velocity V_r to the central line width σ . In this paper we use the term rotation velocity V_r to refer to the measured projection of the circular velocity V_c . For an edge-on galaxy $V_r = V_c$. For a galaxy with angle of inclination $i < 90^\circ$, the ratio V_r/V_c depends on i , as well as the alignment of the slit relative to the major axis. The angular displacement from the galaxy centre at which V_r is measured, θ , is listed in col. (7), and the corresponding projected distance, r , is listed in col. (8)¹. The last three columns list the slit width

¹ In this paper we use the symbol r for projected radius, and R for deprojected radius.

Table 1. Table of line widths of LBGs measured from rest-frame optical emission lines

Galaxy	z	\mathcal{R}	σ (km s^{-1})	line	ref.
(1)	(2)	(3)	(4)	(5)	(6)
CDFa D18	3.1122	23.74	79 ± 7	[O III]	P01
CDFa C8	3.0752	23.72	106 ± 6	[O III]	P01
CDFa C1	3.1147	23.53	≤ 63	[O III]	P01
Q0201+113 C6	3.0548	23.92	64 ± 4	[O III]	P01
Q0256-000 C17	3.2796	23.89	53 ± 4	[O III]	P01
Q0347-383 C5	3.2337	23.82	69 ± 4	[O III]	P01
B2 0902+343 C12	3.3866	23.63	87 ± 12	[O III]	P01
West MMD11	2.9816	24.05	53 ± 5	[O III]	P01
Q1422+231 D81	3.1037	23.41	116 ± 8	[O III]	P01
3C324 C3	3.2876	24.14	76 ± 18	[O III]	P01
SSA22a MD46	3.0855	23.30	67 ± 6	[O III]	P01
SSA22a D3	3.0687	23.37	113 ± 7	[O III]	P01
DSF 2237+116a C2	3.3176	23.55	100 ± 4	[O III]	P01
Q0000-263 D6	2.966	22.88	60 ± 10	[O III]	P01
B2 0902+343 C6	3.091	24.13	55 ± 15	[O III]	P01
MS1512-cB58	2.7290	24.10	81	[O III]	P01
CDFb-BN88	2.2615	23.14	96 ± 46	H α	E03
Q0201-B13	2.1663	23.34	62 ± 29	H α	E03
Westphal-BX600	2.1607	23.94	181 ± 24	H α	E03
Q1623-BX376a	2.4085	23.31*	261 ± 72	H α	E03
Q1623-BX376b	2.4085		< 224	H α	E03
Q1623-BX432	2.1817	24.58	51 ± 22	H α	E03
Q1623-BX447	2.1481	24.48	174 ± 18	H α	E03
Q1623-BX449	2.4188	24.86	141 ± 94	H α	E03
Q1623-BX511	2.2421	25.37	152 ± 47	H α	E03
Q1623-BX522	2.4757	24.50	< 44	H α	E03
Q1623-MD107	2.5373	25.35	< 42	H α	E03
Q1700-BX691	2.1895	25.33	170 ± 18	H α	E03
Q1700-BX717	2.4353	24.78	< 60	H α	E03
Q1700-MD103	2.3148	24.23	75 ± 21	H α	E03
Q1700-MD109	2.2942	25.46	87 ± 35	H α	E03
SSA22a-MD41	2.1713	23.31	107 ± 15	H α	E03

* Q1623-BX376 appears as a single extended object for photometry but is resolved into two lines at the same redshift in the H α spectroscopy (see E03 for further details).

of the spectroscopic measurement (col. 9), the emission line measured (col. 10), and the reference (col. 11).

An important point to note is that, with one exception, the usual procedure of aligning the slit with the galaxy major axis was not followed for these galaxies. In most cases this was because only ground-based imaging was available at the time of the spectroscopic observations, and therefore there was no useful information on the galaxy orientations. Therefore, in the analysis of rotation velocities (Section 3), we assume a random angle of the slit relative to the galaxy major axis. The one exception is the galaxy SSA22a-MD41. This galaxy is included in Table 2 for completeness, but is excluded from the analysis. The number of galaxies used in the analysis of rotation is seven, therefore.

3 ANALYSIS OF ROTATION CURVES

In this section we analyse the kinematic data for this small subsample of seven LBGs. The aim is to investigate the relation between the two quantities σ and V_r . Rotation velocities are more difficult to measure, requiring detection of emission lines in the fainter outer parts of galaxies. Also, rotation velocities measure only the projection of the useful quantity, the circular velocity V_c . Since the inclination angles of LBGs cannot be measured reliably, data on rotation velocities require a statistical analysis. The central line widths, on the other hand, are easier to measure, and, to

the extent that they reflect random motions rather than rotation, provide the kinematic quantity of interest (i.e. the one-dimensional velocity dispersion) directly. The disadvantage, as stated earlier, is that the measurements are confined to small radii. Therefore the purpose of our analysis is to see whether the line width can be used as a predictor of the circular velocity.

What do the central line widths of LBGs represent? The results of a similar analysis of the kinematics of nearby starburst galaxies, by Lehnert & Heckman (1996), bear comparison. These authors plotted [NII] nuclear line width against galaxy circular velocity, and found no correlation. However it is not clear how relevant this analysis is to the measurements of LBGs. Lehnert & Heckman suggested that the lack of correlation was because their nuclear measurements, scale 1 arcsec at $z \sim 0.05$, $\equiv 0.1\text{kpc}$, sample the steeply rising part of the rotation curve. In contrast the line widths of LBGs sample larger radii, scale 0.2 arcsec at $z \sim 3$, $\equiv 1.5\text{kpc}$, and characterise the motion of the majority of the luminous matter in the galaxies. All the same, the central line widths may not reflect random motions, but could include a contribution from rotation. Rather than attempt to interpret exactly what the central line widths measure, or, indeed, to relate the results at high redshift to the results at low redshift, we simply ask the question whether the central line widths are useful.

The answer to this question is provided by Fig. 1, where we plot, as the stepped solid line, the cumulative probability distribution function (PDF) of the ratio V_r/σ for the seven galaxies with measured rotation velocities. Testing the MMW picture hinges on a careful interpretation of this figure. To aid the interpretation we have computed the predicted cumulative PDFs for some simple models. In these models we suppose galaxies may be approximated as stellar disks of negligible mass embedded in dark matter singular isothermal spheres (SIS), characterised by the one-dimensional velocity dispersion, σ_{1D} . The SIS has a flat rotation curve, and the circular velocity is related to the one-dimensional velocity dispersion by $V_c = \sqrt{2}\sigma_{1D}$. The dashed curves (1) and (2) in Fig. 1 are the predicted cumulative PDFs of the ratio V_r/σ_{1D} for the limiting cases (1) where the galaxy is much larger than the slit width (the “large-galaxy case”), and (2) where the galaxy is smaller than the slit width (the “small-galaxy case”). For the small-galaxy case, the curve is shifted to higher values of V_r/σ_{1D} relative to the large-galaxy case. This is because, in the small-galaxy case, the emission from material along the galaxy major axis, which has the highest rotation velocity, is always recorded, whereas in the large-galaxy case this only occurs when the slit is fortuitously aligned along the major axis.

Before attempting to interpret these results we quantify the goodness of fit between the data and the models, with the Kolmogorov-Smirnov (KS) test. For the large-galaxy case we find a KS probability $P(KS) = 0.01$, and for the small-galaxy case we find $P(KS) = 0.36$. The dotted curve (3), in Fig. 1, is an intermediate case, where, for each value of V_r/σ_{1D} , we have averaged the cumulative probabilities for cases (1) and (2). For curve (3) we find $P(KS) = 0.42$. Curves (2) and (3) are therefore consistent with the data, while curve (1) is inconsistent with the data.

To interpret the stepped line, we begin with the hypothesis that the circular velocity in any galaxy may be

Table 2. Summary of rotation velocity data for LBGs

Galaxy	z	\mathcal{R}	σ (km s ⁻¹)	V_r (km s ⁻¹)	V_r/σ	θ (arcsec)	r (kpc)	slit width (arcsec)	line	ref.
(1)	(2)	(3)	(4)	(5)	(6)	(7)	(8)	(9)	(10)	(11)
Q0347-383 C5	3.2337	23.82	69 ± 4	31	0.45	0.60	4.5	1.0	[O III]	P01
SSA22a MD46	3.0855	23.30	67 ± 6	40	0.60	0.59	4.5	1.0	[O III]	P01
Westphal-BX600	2.1607	23.94	181 ± 24	210	1.16	0.71	5.9	0.76	H α	E03
Q1623-BX447	2.1481	24.48	174 ± 18	160	0.92	0.61	5.1	0.76	H α	E03
Q1623-BX511	2.2421	25.37	152 ± 47	80	0.53	0.38	3.1	0.76	H α	E03
Q1700-BX691	2.1895	25.33	170 ± 18	220	1.29	0.76	6.3	0.76	H α	E03
Q1700-MD103	2.3148	24.23	75 ± 21	100	1.33	0.84	6.9	0.76	H α	E03
SSA22a-MD41*	2.1713	23.31	107 ± 15	150	1.40	0.98	8.1	1.0	H α	E03

* SSA22a-MD41 is not used in the statistical analysis of rotation curves as the slit was intentionally aligned along the galaxy major axis.

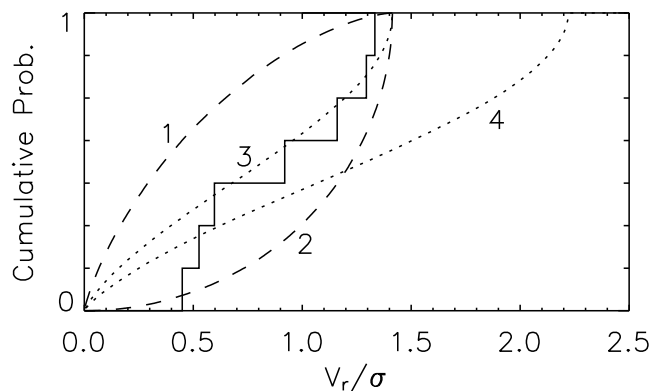
predicted using the relation $V_c = \sqrt{2}\sigma$. [Note, however, that, at this stage, we make no attempt to connect the quantity σ (measured from the LBG line widths) and the quantity σ_{1D} .] Under this hypothesis, the predicted cumulative PDF for V_r/σ depends on the size of the galaxies relative to the slit, and would lie between curves (1) and (2). Since the projected angular diameters of the galaxies (average value $2\theta = 1.3''$, Table 2) are comparable to, but a little larger than, the slit width, if the hypothesis $V_c = \sqrt{2}\sigma$ is a good one, we would expect the data to lie closer to curve (2) than to curve (1), and therefore somewhere between curves (3) and (2). Since the data do indeed fall between curves (3) and (2), and since the KS probabilities for these two curves are both satisfactory, we conclude that the data are consistent with the hypothesis $V_c = \sqrt{2}\sigma$.

Since this conclusion is based on a small sample, to what extent could this relation underestimate the galaxy circular velocities? We will establish this by stretching the intermediate curve by a factor F . In other words if we apply the relation $V_c = F\sqrt{2}\sigma$, how large can F be before the intermediate curve no longer matches the data? Because the circular velocities predicted by MMW are large, in the context of ruling out the MMW model this is a conservative assumption, since we should really stretch a curve that lies between (3) and (2), in which case the factor F would be smaller. We find that when $F = 1.55$ the probability $P(\text{KS})$ falls to 0.05, which is to say that the relation $V_c = \sqrt{2}\sigma$ underestimates the circular velocities by 55 percent, at the most. This stretched curve is plotted as curve 4 in Fig. 1.

Turning to the physical meaning of these results, one possible interpretation is that the mass distribution in the central few kpc of LBGs is approximately isothermal i.e. their rotation curves are approximately flat. While this is perfectly plausible, this interpretation relies on the identification of σ with σ_{1D} , in other words that the line widths reflect random motions as opposed to rotation (or indeed any non-gravitational motions). Higher resolution spectroscopic data, from adaptive-optics fed spectrographs, will be required to confirm this conjecture. For our purposes, however, it is sufficient to note simply that a good fit to the distribution of rotation velocities for these seven galaxies is obtained by applying the relation $V_c = \sqrt{2}\sigma$, which is to say that, for a sample of LBGs, the distribution of central line widths is a good predictor of the distribution of the circular velocities at radii of several kpc. This may or may not be true for individual galaxies.

The galaxies of Table 2 are the subsample of galaxies

Figure 1. Cumulative PDFs of the ratio V_r/σ for the seven galaxies from Table 2 (excluding SSA22a-MD41) plotted solid, and for four models. Dashed: (1) SIS large-galaxy case, (2) SIS small-galaxy case. Dotted: (3) SIS intermediate case (average of lines 1 and 2), (4) intermediate case stretched by a factor $F = 1.55$.



in Table 1 for which it was possible to measure rotation i.e. for which ionised gas is detectable a few kpc from the galaxy centre. For the present we assume this subsample provides an unbiased estimate of the quantity V_c/σ , and we will apply the relation $V_c = \sqrt{2}\sigma$ to all the galaxies of Table 1. Possible biases are discussed in Section 4. Since the quantity V_c/σ is a dimensionless ratio it is unlikely to be a strong function of luminosity or redshift, so even if the galaxies in the subsample of Table 2 differed substantially from the galaxies of Table 1 in terms of these quantities, one might reasonably still apply the relation. In fact the two samples are quite well matched. For the seven galaxies with rotation measures the average quantities are $\overline{\mathcal{R}} = 24.4$, and $\overline{z} = 2.48$, and for the galaxies in Table 1 the average quantities are $\overline{\mathcal{R}} = 24.1$, and $\overline{z} = 2.71$.

The average projected radius at which the rotation velocity was measured for the seven galaxies used in the analysis of this section (Table 2) is $\overline{r} = 5.2$ kpc. Accounting for projection effects, this corresponds to an average deprojected radius of $\overline{R} \sim 7$ kpc. In the following section we compare the distribution of circular velocities at a radius of 7 kpc predicted by MMW, for the dark matter, against the distribution of circular velocities at that radius inferred for the galaxies of Table 1, by applying the relation $V_c = \sqrt{2}\sigma$.

4 COMPARISON AGAINST THEORETICAL PREDICTIONS

In this section we first summarise the predictions of MMW of the halo circular velocities of LBGs, and then compare these predictions against the data of Table 1. Specifically the MMW predictions are for LBGs at $z = 3$, brighter than $\mathcal{R} = 25.5$. Using the luminosity function provided by Adelberger and Steidel (2000), the average magnitude of this population is $\overline{\mathcal{R}} = 24.9$. The average quantities for the observed galaxies in Table 1 are $\overline{z} = 2.71$ and $\overline{\mathcal{R}} = 24.1$. Therefore the average redshift of the observed galaxies is quite close to the comparison datum $z = 3$, while the average apparent magnitude is brighter by 0.8 mag. One might expect a sample of galaxies with average apparent magnitude $\overline{\mathcal{R}} = 24.9$ to have smaller circular velocities on average than the sample of Table 1. All the same P01 found no correlation between central line width and galaxy luminosity in their sample.

MMW begin with the assumption that LBGs are the central galaxies of the most massive dark-matter halos. The Press-Schechter formalism yields the mass function, and the density profiles are assumed to be of NFW form (Navarro et al., 1997). In outline, matching to the observed volume density of LBGs brighter than $\mathcal{R} = 25.5$, provided by Adelberger et al. (1998), specifies the distribution of halo circular velocities², which is plotted in fig. 4 of MMW (the solid line plots the results for the Λ cosmology adopted in this paper). Here the halo circular velocity V_h is the value at the virial radius R_h , which is the radius at which the average density of the halo inside that radius is equal to 200 times the critical density at that epoch, $\rho_c = 3H(z)^2/(8\pi G)$. Therefore V_h and R_h are simply related by $V_h = 10H(z)R_h$. Note that the halo mass $M_H = V_h^2 R_h/G$, is proportional to V_h^3 .

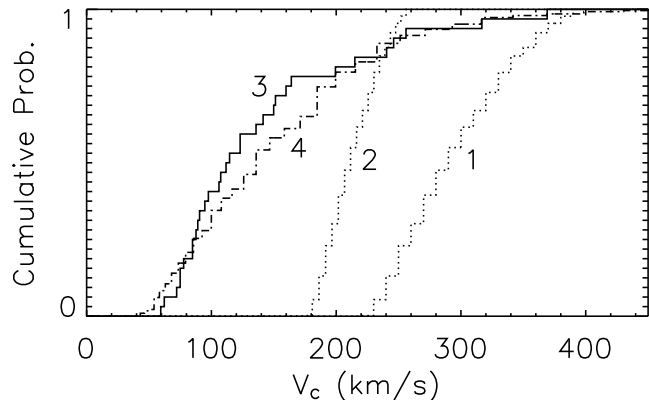
For the NFW profile, the circular velocity V_c at any radius, specified by $x = R/R_h$, is related to V_h by:

$$\left(\frac{V_c}{V_h}\right)^2 = \frac{1}{x} \frac{\ln(1+cx) - (cx)/(1+cx)}{\ln(1+c) - c/(1+c)}.$$

Here the parameter c , called the ‘concentration’, is the ratio R_h/R_s , where R_s is the scale radius of the NFW profile. The typical predicted halo circular velocities are in the range 200–400 km s⁻¹. Based on the results of Zhao et al. (2003), a suitable value for the concentration at $z \sim 3$, for these values of V_h , is $c = 4$ (Mo, priv. comm.). Using this value we can now compute the ratio V_c/V_h at the radius of interest $R = 7$ kpc, for different values of V_h , and transform the distribution of V_h to the distribution of V_c . For example, for halo circular velocities of 200 and 400 km s⁻¹, we find $V_c/V_h = 0.81$ and 0.64, respectively.

In Fig. 2 we compare the predicted circular velocities of LBGs against the measured values. In this plot line (1) shows the cumulative distribution of V_h , predicted by MMW, and line (2) shows the cumulative distribution of V_c at $R = 7$ kpc, computed as described above. Line (3) is the cumulative distribution of measured circular velocities of LBGs at $R = 7$ kpc, produced by applying the relation $V_c = \sqrt{2}\sigma$ to the data of Table 1. The measured circular velocities are much smaller than the predicted values. The probability that the two distributions are drawn from the same population

Figure 2. Measured and predicted cumulative PDFs of the circular velocity of LBGs at $z = 3$: Line (1) MMW prediction for V_h , line (2) MMW prediction for V_c at $R = 7$ kpc, line (3) measured values of V_c at $R = 7$ kpc for the 32 galaxies of Table 1, derived using the relation $V_c = \sqrt{2}\sigma$, line (4) SPF collisional starburst prediction for V_c .



is negligible. Allowing for appropriate scatter in the parameter c does not alter this conclusion. We have computed the scaling by which the circular velocities of line (2) should be divided, to provide the best fit to line (3), as measured by the KS test. This factor, which we call Q , is 1.8. We can associate an indicative 1σ uncertainty of 0.4 with this factor, by recalling the results of Section 3, where we found that, at 5 percent confidence (i.e. 1.65σ), the relation $V_c = \sqrt{2}\sigma$ could underestimate the true circular velocities by a factor as large as $F = 1.55$. To summarise, we find that the circular velocities at a radius $R = 7$ kpc, predicted by MMW, are a factor $Q = 1.8 \pm 0.4$ larger than the measured circular velocities of LBGs at $z \sim 3$. This rather large uncertainty in Q is a consequence of: i) the small number of galaxies with rotation measures, ii) the fact that the slit was not aligned along the major axis, but fell at a random angle.

Could this discrepancy between the predicted and measured circular velocities of LBGs be explained by a bias in the data? E03 note one such effect. For the small-galaxy case, at any particular projected radius, the line flux includes contributions both from the point on the galaxy major axis (where the rotation velocity is a maximum), and from points off the major axis (where the rotation velocities are smaller). For this reason some of the rotation velocities measured by Erb may be smaller than the true values, and this would reduce the discrepancy between theory and observation. This effect is mitigated to some extent by the falling surface brightness profiles of galaxies, since at any projected radius the surface brightness is then highest along the major axis. Another effect which we have not considered acts in the opposite sense, and widens the discrepancy between theory and observation. For galaxies larger than the slit width, the projected radius of the flux in the slit is largest when the slit is aligned along the major axis. These are also the galaxies (for the given inclination angle) for which the measured rotation velocity is maximised. For galaxies oriented away from the slit, the projected radius will be smaller, and then the elongation along the slit may not be detectable. These galaxies have smaller rotation velocities, and may be missing from the sample. Indeed it is noticeable that there are no LBGs in Table 2 for which $V_r/\sigma < 0.4$. To test this we

² The actual model is more detailed than implied here.

made a simple simulation of galaxies of radius ~ 1 arcsec, with random inclination angles, and observed in 0.5 arcsec seeing, at random slit positions. We discarded objects with projected size along the slit smaller than the seeing. The simulated curve closely follows the stepped line in Figure 1, the limit on the projected size causing the dearth of objects with small rotation velocities. This indicates that the apparent deficit visible in Fig. 1 may be a selection effect. If so the factor F computed above (and so the uncertainty on Q also) will have been overestimated.

There are number of other reasons to believe that the discrepancy between theory and observation, may be more significant than estimated above. These include:

(i) The effect of the baryons has not been included in the prediction. Because of dissipation, baryons sink toward the centres of the dark matter halos, deepening the potential well, and raising the circular velocities above the values for the dark matter only.

(ii) In the data of Table 1, where an upper limit to the central line width has been quoted, we have computed the circular velocity for this value, whereas the true circular velocity will be smaller.

(iii) The MMW circular velocities were computed for a population with an average apparent magnitude 0.8 mag. fainter than the average apparent magnitude of the galaxies in Table 1.

(iv) As explained in Section 3, we were conservative in computing the factor F , since to compute F we stretched curve (3) of Fig. 1. A curve between curves (3) and (2) would have produced a smaller value of F , and therefore a smaller value for the uncertainty of Q , increasing the discrepancy between theory and observation.

Taking these factors into consideration, this analysis indicates that the simple model of LBGs marking the centres of the most massive dark matter halos is probably incorrect.

We now consider the alternative picture of LBGs as galaxies brightened by starbursts, triggered by collisions. We take the predicted distribution of halo masses for the SPF collisional starburst model, from Primack et al. (2003), and convert each mass to a circular velocity using equations from the appendix of Somerville and Primack (1999), for the truncated isothermal sphere used in their models. Note that this model has a flat rotation curve and their definition of virial radius differs slightly from that of MMW. The distribution of predicted circular velocities is plotted as line (4) in Fig. 2. The model provides a good fit to the measurements, with associated probability $P(KS)=0.26$. We also computed the circular velocities at $R=7$ kpc assuming an NFW profile, and found values about 10 percent smaller.

It has proved difficult to discriminate between the two models for LBGs at $z \sim 3$ discussed in this paper, on the basis of their luminosities and clustering properties (Wechsler et al., 2001). The evidence assembled here from the kinematics clearly favours the collisional starburst picture. Our analysis has relied on the measurement of rotation velocities for just seven galaxies. Spectroscopic measurements, with high spatial resolution, along the galaxy major axis, for a larger sample, will be useful in further clarifying the nature of LBGs.

ACKNOWLEDGMENTS

We thank Rachel Somerville and Houjun Mo for useful communications regarding the mass distribution of various LBG models. SJW[1] thanks Oliver Warren for his patient mathematical guidance and Thomas Babbedge and Alexander King for their helpful comments on the text.

REFERENCES

- Adelberger K. L., Steidel C. C., Giavalisco M., Dickinson M. E., Pettini M., Kellogg M., 1998, *ApJ*, 505, 18
 Adelberger K. L., Steidel C. C., 2000, *ApJ*, 544, 218
 Babcock H. W., 1939, *Lick Obs. Bull.*, 19, 41
 de Blok W. J. G., Bosma A., McGaugh S., 2003, *MNRAS*, 340, 657
 Erb D. K., Shapley A. E., Steidel C. C., Pettini M., Adelberger K. L., Hunt M. P., Moorwood A. F. M., Cuby J.-G., 2003, *ApJ*, 591, 110
 Giavalisco M., Steidel C. C., Adelberger K. L., Dickinson M. E., Pettini M., Kellogg M., 1998, *ApJ*, 503, 543
 Kolatt T. S. et al., 1999, *ApJ*, 523, L109
 Lacey C., Cole S., 1993, *MNRAS*, 262, 627
 Lehnert M. D., Heckman T. M., 1996, *ApJ*, 472, 546
 Marleau F. R., Simard L., 1998, *ApJ*, 507, 585
 Mo H. J., Mao S., White S. D. M., 1999, *MNRAS*, 304, 175
 Navarro J. F., Frenk C. S., White S. D. M., 1997, *ApJ*, 490, 493
 Pettini M., Shapley A. E., Steidel C. C., Cuby J.-G., Dickinson M., Moorwood A. F. M., Adelberger K. L., Giavalisco M., 2001, *ApJ*, 554, 981
 Primack J. R., Wechsler R. H., Somerville R. S., 2003, in Bender R. & Renzini A., eds. *The Mass of Galaxies at Low and High Redshift. Proceedings of the ESO Workshop held in Venice, October 2001*
 Rubin V. C., Thonnard N., Ford W. K. Jr., 1978, *ApJ*, 225, L107
 Somerville R. S., Primack J. R., 1999, *MNRAS*, 310, 1087
 Somerville R. S., Primack J. R., Faber S. M., 2001, *MNRAS*, 320, 504
 Steidel C. C., Hamilton D., 1993, *AJ*, 105, 2017
 Steidel C. C., Giavalisco M., Pettini M., Dickinson M., Adelberger K. L., 1996, *ApJ*, 462, L17
 Steidel C. C., Adelberger K. L., Dickinson M., Giavalisco M., Pettini M., Kellogg M., 1998, *ApJ*, 492, 428
 van Albada T. S., Bahcall J. N., Begeman K., Sancisi R., 1985, *ApJ*, 295, 305
 Wechsler R. H., Somerville R. S., Bullock J. S., Kolatt T. S., Primack J. R., Blumenthal G. R., Dekel A., 2001, *ApJ*, 554, 85
 Zhao D. H., Mo H. J., Jing Y. P., Börner G., 2003, *MNRAS*, 339, 12

This paper has been typeset from a $\text{\TeX}/\text{\LaTeX}$ file prepared by the author.